

# The princess and the pea

Neil J. Cornish<sup>†</sup> and Norman E. Frankel<sup>‡</sup>

<sup>†</sup>*DAMTP, University of Cambridge, Silver Street, Cambridge CB3 9EW, UK*

<sup>‡</sup>*School of Physics, University of Melbourne, Parkville 3052, Victoria, Australia*

Like a fairy-tale princess, trajectories around black holes can be sensitive to small disturbances. We describe how a small disturbance can lead to erratic orbits and an increased production of gravitational waves.

04.30.Db, 05.45.+b, 97.60.Lf

The high degree of symmetry found in the spacetime of an isolated black hole leads to regular geodesic motion for orbiting bodies. Working on the assumption that small disturbances generally have small effects, it is often tacitly assumed that this idealised, textbook picture carries over to real astrophysical situations. Here we want to emphasise that the idealised picture is not stable against small perturbations, as the non-linearity of Einstein's equations tends to amplify small disturbances.

The observation that small perturbations of an idealised black hole spacetime can lead to qualitative changes in the dynamics is not new. It has previously been noted that a range of perturbations lead to chaotic dynamics. The perturbations considered include additional mass concentrations [1,2,3,4,5], magnetic fields [6], gravitational waves [7] and spin-orbit coupling [8]. Unlike the Kepler problem of Newtonian mechanics, essentially any perturbation of an isolated black hole spacetime will lead to chaotic orbits. This is because even the most pristine black hole spacetime harbours the seeds of chaos in the form of isolated unstable orbits. A small perturbation causes these unstable orbits to break out and infest large regions of phase space. Note that experience with Newtonian systems is very misleading. For example, the Kepler problem has more integrals of motion than are needed for integrability. Keplerian systems are thus impervious to small perturbations. In contrast, black hole spacetimes are at the edge of chaos, just waiting for the proverbial butterfly to flap its wings.

Once it is realised that typical black hole – satellite systems are chaotic in the strong field regime, we are forced to consider the consequences. One of the most immediate consequences is that there will be no such thing as the “last stable orbit” [9]. The boundary between stable and unstable orbits will be fractal, and there may be large fractal tendrils of unstable orbits invading what would have been stable territory in an ideal black hole spacetime. This feature will be important in determining when a binary system switches from inspiral to cataclysmic collapse [9]. Another important consequence will be the increased production of gravitational waves due to the erratic motion of chaotic orbits.

In what follows we will illustrate both of these effects in a simple model system. While our model does not describe a real astrophysical situation, it does capture many

of the salient features we expect to find in a relativistic binary system.

For the purpose of illustration we will study the orbits of non-rotating satellites around an extreme Reissner-Nordstrom black hole. Almost identical results hold for motion around a Schwarzschild black hole perturbed by an orbiting third body [3]. Extreme black holes have the added advantage of allowing an exact generalisation to spacetimes with  $N$  extremal masses [10]. Rotating black holes bring with them a host of new instabilities which only amplify the points we wish to make. Similarly, rotating satellites introduce additional instabilities through spin-orbit [8] and spin-spin couplings. So while our model is chosen on the grounds of simplicity, it is likely that more realistic models will be even more sensitive to small perturbations. Moreover, a central feature of non-linear dynamics is universality: the details of the dynamics are less important than the general structure of the phase space trajectories. For example, a stochastic layer will lead to an increase in the gravitational wave luminosity regardless of what lead to the formation of the stochastic layer. Because of this, the effects we describe for our particular model will enjoy wider applicability.

Our unperturbed spacetime is described by the metric

$$ds^2 = - \left(1 + \frac{M}{r}\right)^{-2} dt^2 + \left(1 + \frac{M}{r}\right)^2 (dr^2 + r^2 d\Omega^2), \quad (1)$$

and electromagnetic potential

$$A_t = \left(1 + \frac{M}{r}\right)^{-1}. \quad (2)$$

Here  $d\Omega^2 = d\theta^2 + \sin^2\theta d\phi^2$  is the metric of a 2-sphere. Into this spacetime we introduce a spinless satellite of mass  $\mu$  and consider its orbits. To keep our model simple we will neglect the spacetime curvature caused by the satellite. The rotational symmetry allows us to restrict our attention to orbits in the plane  $\theta = \pi/2$ . Moreover, invariance under time translations and spatial rotations leads to conservation of the satellite's energy  $\mu E$  and angular momentum  $\mu L$ . This allows the motion to be reduced to the radial equation

$$\left(\frac{dr}{d\tau}\right)^2 = E^2 - V^2(r), \quad (3)$$

where  $\tau$  is the proper time along the trajectory and

$$V(r) = \left(1 + \frac{M}{r}\right)^{-1} \left(1 + \frac{L^2}{(r+M)^2}\right)^{1/2}. \quad (4)$$

We will be concerning ourselves with bound orbits ( $E < 1$ ), but similar conclusions hold for unbound orbits. In Fig. 1 the effective potential  $V(r)$  is displayed for three values of  $L$ . The energy  $E = 0.94$  is also displayed. We see that some orbits can reach the event horizon at  $r = 0$  while others are protected by an angular momentum barrier. For  $E = 0.94$  this occurs at the critical angular momentum  $L_c = 2.982M$ . A trajectory with these parameter values can follow an unstable circular orbit at  $r_c = (L_c^2 - 2M^2 - L_c\sqrt{L_c^2 - 8M^2})/2M$ . As emphasised by many authors, it is the existence of such unstable periodic orbits that make black hole spacetimes sensitive to small perturbations.

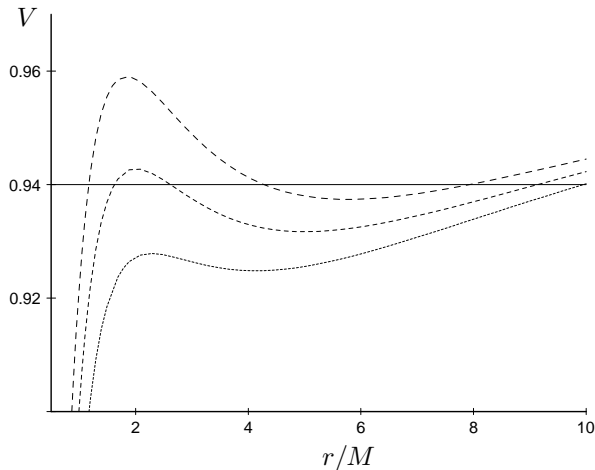


FIG. 1. The effective potential  $V(r)$  for different values of the angular momentum. In order of decreasing height, the potentials correspond to  $L = 3.1M$ ,  $3M$ , and  $2.9M$  respectively. The solid line is the fixed energy  $E = 0.94$ .

Previous studies have used local methods to assess the onset of instability. Here we apply a more revealing global approach based on stability basins. Such global techniques are increasingly being used in engineering applications in order to survey the full range of stable and unstable configurations of circuits, bridges and boats [11]. When systems are chaotic, stable regions of phase space can be invaded by chaotic tendrils. These tendrils exhibit a complicated fractal structure.

To illustrate how small perturbations can lead to important changes in the dynamics we introduce a small ‘‘pea’’ with mass  $m$  and charge  $q = m$  at a distance  $r = R$  from the black hole. The new metric is obtained by replacing  $1 + M/r$  by

$$U = 1 + \frac{M}{r} + \frac{m}{\sqrt{R^2 - 2Rr \cos \phi + r^2}}, \quad (5)$$

leading to

$$ds^2 = U^2 (E^2 d\tau^2 + dr^2 + r^2 d\theta^2 + \sin^2 \theta d\phi^2). \quad (6)$$

The new metric is an exact solution to the Einstein-Maxwell field equations belonging to the Majumdar-Papapetrou [10] family of spacetimes. The leading corrections to the extreme Reissner-Nordstrom metric are given by

$$\Delta U = \frac{m}{R} \left(1 + \frac{r}{R} \cos \phi + \frac{r^2}{2R^2} [3 \cos^2 \phi - 1] + \dots\right). \quad (7)$$

The dipole term,  $\cos \phi$ , can be removed by a coordinate transformation, while the quadrupole term,  $(3 \cos^2 \phi - 1)$ , is analogous to a perturbation of the Schwarzschild metric studied by Moeckel [3]. He described how a small body orbiting a Schwarzschild black hole causes the inner orbits to become chaotic.

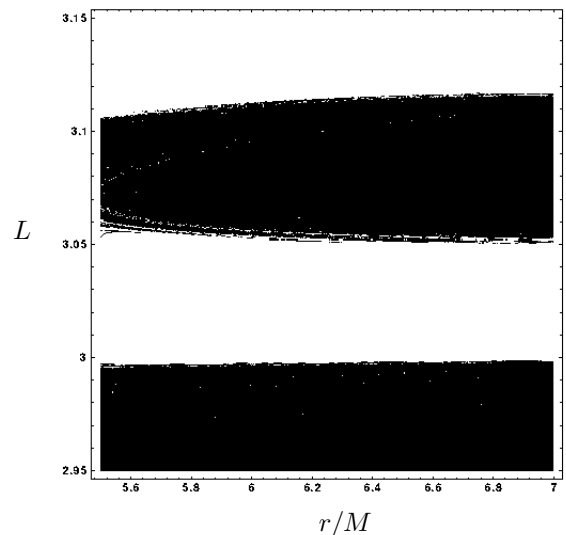


FIG. 2. Basin boundaries in the  $(L, r)$  plane.

Since our perturbed metric is static, the satellite’s energy remains a conserved quantity. In addition, the modified potential is independent of  $\theta$ , so  $p_\theta$  is conserved. This means we can continue to study trajectories in the plane  $\theta = \pi/2$  without loss of generality. However, the  $\phi$  dependence of the potential breaks rotational invariance so the satellite’s angular momentum is no longer conserved. A trajectory with  $L(0) > L_c$  can now evolve to one with  $L(\tau) < L_c$ , thus allowing the possibility of capture by the black hole. Conversely, a trajectory that was destined for capture might now gain enough angular momentum to avoid capture. For chaotic trajectories

this gain or loss of angular momentum can depend sensitively on initial conditions, leading to complicated fractal boundaries separating the stable and unstable outcomes.

Here we are working under the usual assumption that we can use the dynamics of the dissipationless system to predict which orbits will be unstable when gravitational radiation is included as a form of dissipation. This amounts to a kind of adiabatic approximation which is valid when the energy loss per orbit is much less than the energy of the satellite.

In Fig. 2 we display the stability basin in the  $(L, r)$  plane for a particle with energy  $E = 0.94$ . A small pea with mass  $m = M/100$  has been introduced at  $r = R = 10M$ . Particles are started from an initial position  $r$ , with “angular momentum”  $L = r^2 U^2 d\phi/d\tau$ . The trajectory is then evolved numerically. If the particle is captured by the black hole we colour the initial position white. If the particle achieves a stable orbit (defined here to be 100+ orbits without being captured), then we colour the initial position black. There are two major features of note in Fig. 2. The first is the irregular boundaries between stable and unstable outcomes. The second is the broad swath of unstable trajectories between  $L = 3M$  and  $L = 3.15M$ . Before the pea was introduced, all trajectories with  $L > L_c = 2.982M$  were stable.

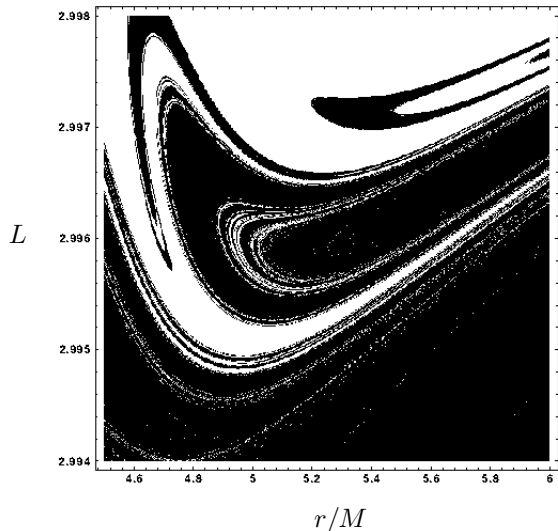


FIG. 3. A detail of Fig. 2 near  $L = L_c$ .

The stability basins for the unperturbed spacetime are separated by a smooth line at  $L = L_c$ . In Fig. 3 we display a detail of Fig. 2 which clearly shows that the smooth boundary near  $L_c$  has been replaced by a complicated fractal structure. Note that most orbits with  $L < 2.995M$  have been rendered unstable and thrown into the black hole. In Fig. 4 we see that the central basin of instability also has a fractal boundary. Fractal structures provide a gauge invariant signal of chaos in general relativity [4,12,13].

But aside from producing nice pictures, what does chaos add to the physics of satellites orbiting black holes? One interesting possibility is an enhancement of the gravitational wave output. Chaotic trajectories will tend to produce gravitational waves with increased luminosity and amplitude, and erratic variations in amplitude. The power radiated will exceed that of stable orbits since, in loose terms, the luminosity is proportional to the rate of change of acceleration. Chaotic orbits often exhibit highly variable accelerations while nearly circular orbits have gently varying acceleration profiles. In fact, even elliptical orbits produce considerably more gravitational radiation than circular orbits due to the sharp turn at their point of closest approach. Unfortunately, most orbits are expected to be nearly circular by the time they reach their swan song in the LIGO detection band [14]. This is because tidal friction and gravitational radiation act to circularise the orbit. To get more powerful gravitational wave signals we need something to destabilise this picture. Enter chaotic resonances.

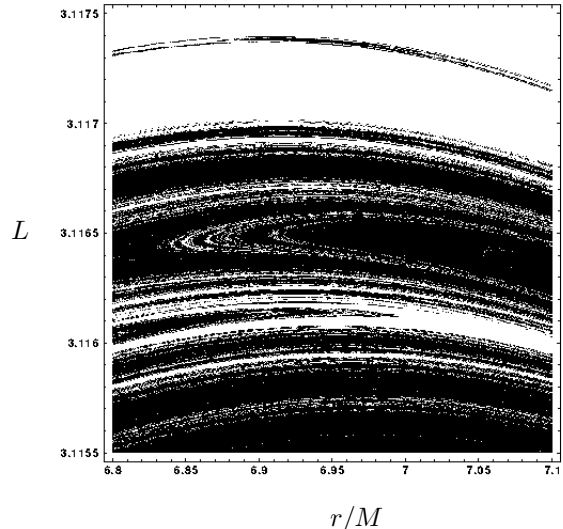


FIG. 4. A detail of Fig. 2 showing the boundary of the band of instability.

As a realistic binary system spirals inwards, various relativistic instabilities start to become important. The instabilities might be caused by spin-orbit or spin-spin coupling, or by external mass distributions such as the third body studied here. While these resonances are typically restricted to isolated bands in phase space, the inspiralling satellite is likely to run across an unstable band as its energy and angular momentum are reduced by the emission of gravitational waves. The resulting chaotic orbit would then provide a boost to the gravitational wave output.

To get a feel for this chaotic enhancement we can calculate the wave amplitude and power radiated using the quadrupole approximation. Since the orbits we are

studying are fairly relativistic, the quadrupole approximation can only provide a qualitative picture. The power radiated by the satellite is given by [15]

$$P = \frac{1}{5} \langle (d_t^3 I_{ij})^2 \rangle, \quad (8)$$

where  $\langle \rangle$  denotes the average over several orbits and  $I_{ij}$  is the reduced quadrupole moment of the satellite's orbit ( $i, j = 1, 2, 3$ ):

$$I_{ij} = (x_i x_j - \frac{1}{3} r^2) \mu. \quad (9)$$

The notation  $d_t^3$  is shorthand for  $d^3/dt^3$ . The direction-averaged wave amplitude is given by

$$A \propto \sqrt{(d_t^2 I_{ij})(d_t^2 I^{ij})}. \quad (10)$$

Switching to cartesian coordinates, and considering orbits in the plane  $z = 0$  ( $\theta = \pi/2$ ) we find

$$A \propto (3(d_t^2(xy))^2 + [d_t^2 x^2 - d_t^2 y^2]^2 + (d_t^2 x^2)(d_t^2 y^2))^{1/2}.$$

In Fig. 5 we display the amplitude of three representative trajectories with  $E = 0.94$ , normalised against the stable circular orbit of the unperturbed system with  $L = 3.1518M$ .

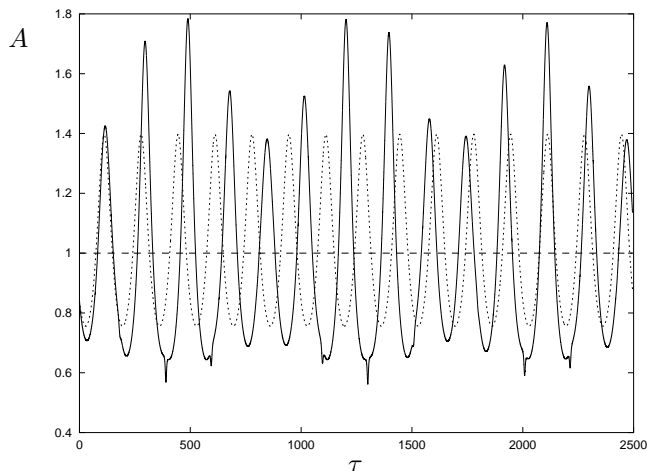


FIG. 5. The amplitude of circular (dashed line), elliptic (dotted curve) and mildly chaotic (solid curve) satellite orbits.

The dotted line shows the variation in amplitude of a precessing elliptical orbit of the unperturbed system with  $L = 3.117M$ . The solid line is for an orbit with the same initial conditions as the regular elliptic orbit, but this time for the perturbed system. The variation in amplitude is increased by up to a factor of two over the unperturbed system. The elliptic and chaotic orbits have power outputs 1.48 and 2.01 times larger than the stable circular orbit. This implies that the small perturbation caused by the ‘‘pea’’ increased the power output by 36%.

To better assess the significance of this result, we need to understand the types of trajectories that give rise to increased power output, how generic these might be in physically reasonable spacetimes and how large the effect can be. To this end, we display in Fig. 6 a Poincaré section for trajectories with  $E = 0.94$ . The Poincaré section reveals a combination of unbroken KAM tori, island chains, cantori and thin stochastic layers. These features are typical for mildly chaotic systems. The chaotic orbit shown in Fig. 5 forms the thin stochastic layer that makes up the outermost ring of the Poincaré section. While this orbit is amongst the most chaotic we found, it only ergodically wanders over a very small band in phase space. The unbroken KAM tori prevent orbits from becoming highly erratic. This in turn limits the gravitational wave output. Moreover, orbits of the perturbed system that lie on the unbroken KAM tori experience much smaller increases in power output. For example, the outermost unbroken KAM tori in Fig. 6 produces just 5% more power than the analogous orbit of the unperturbed spacetime.

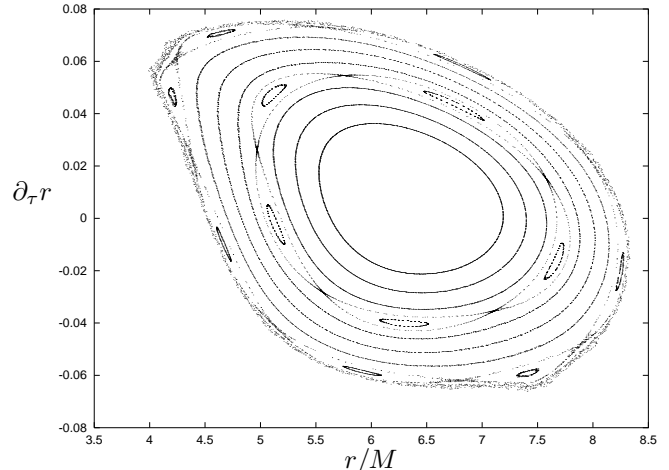


FIG. 6. A Poincaré section for trajectories with  $E = 0.94$ .

These observations suggest that the power output is greatest for orbits that fill the largest regions of phase space. In the model spacetime we have been studying the dynamics is dominated by unbroken KAM tori, and this limits the size of any stochastic layers. In addition, we studied a 4-dimensional Hamiltonian system so the unbroken KAM tori partition phase space. Systems with fewer KAM tori, higher dimensional dynamics, and/or dissipation typically have trajectories that wander over large regions of phase space. In such systems the effects we have been describing will be larger and more widespread.

The literature already contains several realistic black hole models where highly erratic orbits have been found. For example, some of the trajectories shown in Fig. 1 of Ref. [5], and Fig. 4(f) of Ref. [8] form wide stochastic layers. We are currently modelling these spacetimes to

see how large the gravitational wave enhancement can be.

Using a simple model we have shown that chaotic instabilities will affect a satellite's transition from inspiral to plunge, and cause an increase in gravitational wave production. Both of these features could be important when producing gravitational wave templates for the LIGO and LISA detectors.

We thank Sam Drake, Eric Poisson and Janna Levin for informative discussions. This work was supported by the Australian Research Council.

- 
- [1] S. Chandrasekhar, Proc. R. Soc. London **A421**, 227 (1989).
  - [2] G. Contopoulos, Proc. R. Soc. London **A431**, 183 (1990); **A435**, 551 (1991).
  - [3] R. Moeckel, Commun. Math. Phys. **150**, 415 (1992).
  - [4] C. P. Dettmann, N. E. Frankel & N. J. Cornish, Phys. Rev. D**50**, R618 (1994); Fractals **3**, 161 (1995);
  - [5] W. M. Vieira & P. S. Letelier, Phys. Rev. Lett. **76**, 1409 (1996).
  - [6] V. Karas & D. Vokrouhlicky, Gen. Rel. Grav. **24**, 729 (1992).
  - [7] L. Bombelli & E. Calzetta, Class. Quant. Grav. **9**, 2573 (1992).
  - [8] S. Suzuki & K. Maeda, preprint gr-qc/9604020 (1996).
  - [9] L. E. Kidder, C. M. Will & A. G. Wiseman, Phys. Rev. D**47**, 3281 (1993).
  - [10] S. D. Majumdar, Phys. Rev. **72**, 390 (1947), A. Papapetrou, Proc. R. Irish Acad. **A51**, 191 (1947), J. B. Hartle & S. W. Hawking, Commun. Math. Phys. **26**, 87 (1972).
  - [11] J. M. T. Thompson & H. B. Stewart, *Nonlinear Dynamics and Chaos*, (Wiley, Chichester, 1986), M. Kan & H. Taguchi, in *Towards the Harnessing of Chaos*, M. Yamaguti ed., (Elsevier, Amsterdam, 1994).
  - [12] S. P. Drake, C. P. Dettmann, N. E. Frankel & N. J. Cornish, Phys. Rev. E**53**, 1351 (1996).
  - [13] N. J. Cornish & J. J. Levin, Phys. Rev. D**53**, 3022 (1996); Phys. Rev. Lett. **78**, issue 6, (1997).
  - [14] A. Abromovici *et al.*, Science **256**, 325 (1992).
  - [15] L. D. Landau & E. M. Lifshitz, *The Classical Theory of Fields*, (Pergamon Press, 1951).